Boundary layer flow and heat transfer of a Casson fluid past a symmetric porous wedge with surface heat flux

Swati Mukhopadhyay[†] and Iswar Chandra Mandal[‡]

Department of Mathematics, The University of Burdwan, Burdwan-713104, W. B., India

(Received 23 May 2013; revised manuscript received 14 July 2013; published online 20 February 2014)

The aim of this paper is to investigate numerically the boundary layer forced convection flow of a Casson fluid past a symmetric porous wedge. Similarity transformations are used to convert the governing partial differential equations into ordinary ones. With the help of the shooting method, the reduced equations are then solved numerically. Comparisons are made with the previously published results in some special cases and they are found to be in excellent agreement with each other. The results obtained in this study are illustrated graphically and discussed in detail. The velocity is found to increase with an increasing Falkner–Skan exponent whereas the temperature decreases. With the rise of the Casson fluid parameter, the fluid velocity increases but the temperature is found to decrease in this case. Fluid velocity is suppressed with the increase of suction. The skin friction decreases with the increasing value of Casson fluid parameter. It is found that the temperature decreases as the Prandtl number increases and thermal boundary layer thickness decreases with the increasing value of Prandtl number. A significant finding of this investigation is that flow separation can be controlled by increasing the value of the Casson fluid parameter as well as by increasing the amount of suction.

Keywords: symmetric wedge, Casson fluid, heat flux, suction/blowing

PACS: 47.15.Cb, 47.50.−d, 44.20.+b **DOI:** 10.1088/1674-1056/23/4/044702

1. Introduction

During the last few decades, boundary layer theory has been used successfully in the case of non-Newtonian fluid and the boundary layer flows of non-Newtonian fluids have become an interesting topic of investigation as it has vast applications in different industries. As the fluids are very complex in nature, no single constitutive equation exhibiting all properties of such fluids is available.[1,2] Several models can be found in this regard. As the governing equations of non-Newtonian fluids are highly nonlinear and much more complicated than those of Newtonian fluids, much care is needed in investigating such fluids for the understanding of the flow characteristics of a non-Newtonian fluid.[3,4] Non-Newtonian power-law model is vastly used in the literature. Simply because these fluids are mathematically easiest to treat among most of the non-Newtonian fluids.[5] There are other non-Newtonian models as well, for example, Casson fluid model. In the literature, the Casson fluid model is sometimes stated to fit the rheological data, and it is better than general viscoplastic models for many materials. It becomes the preferred rheological model for blood and chocolate. Casson fluid exhibits a yield stress. If a shear stress less than the yield stress is applied to the fluid, it behaves like a solid whereas if a shear stress greater than the yield stress is applied, it starts to move.[6,7]

During the last few decades, laminar boundary-layer flow past a semi-infinite wedge is of considerable practical and theoretical interest. Falkner and Skan[8] investigated numerically the steady incompressible laminar boundary-layer flow past a wedge. Hartree,[9] Hady and Hassanien[10] further studied the problem in detail. The process of suction and blowing has also its importance in many engineering activities, for example, in the design of thrust bearing and radial diffusers, and thermal oil recovery. Keeping this in mind, Lin H T and Lin L K[11] reported on the effect of a transverse magnetic field on a permeable symmetric wedge in a non-Newtonian fluid. Later on, Watanabe and Pop[12] presented numerical results for MHD free convection flow of a Newtonian fluid over a wedge. Kafoussias and Nanousis[13] investigated the MHD laminar boundary-layer flow of a non-Newtonian fluid over a permeable wedge. Yih[14] analyzed the MHD forced convection flow adjacent to a non-isothermal wedge. Wedge flow problem under various thermo-physical conditions was considered by several researchers viz. Hossain *et al.*,[15] Chamkha *et al.*,[16] Pantokratoras,[17] Mukhopadhyay,[18] Pal and Mondal,[19] and others. As is well known, suction is applied to chemical processes to remove reactants whereas blowing is used to add reactants, cool the surface, prevent corrosion or scaling and reduce the drag. Motivated by this, Kandasamy *et al.*[20] presented the influence of chemical reaction on flow passing through a permeable wedge. Also, Hossain *et al.*[21] studied the unsteady boundary-layer flow passing through a wedge. The problems with variable surface heat flux have been introduced in many other studies. Kim,[22] and Kim and Kim[23] have considered the steady boundary-layer flow of a micropolar fluid passing through a fixed wedge with a constant surface temperature and constant surface heat flux, respectively. Later on, the MHD micropolar fluid flow past a

[†]Corresponding author. E-mail: swati_bumath@yahoo.co.in
[‡]Corresponding author. E-mail: iswar.chandra2010@gmail.com

© 2014 Chinese Physical Society and IOP Publishing Ltd

wedge in the presence of uniform heat flux was considered by Ishak *et al.*[24] Riley and Weidman,[25] and Ishak *et al.*[26,27] extended the boundary layer flow over a static or a moving wedge in a viscous fluid (regular fluid) under diverse physical aspects. Kandasamy *et al.*[28] reported on the combined effects of variable viscosity, thermophoresis, and chemical reaction on mixed convection flow past a porous wedge embedded in a non-Darcy porous medium. Recently, in the case of a nanofluid, Yacob *et al.*[29] analyzed the static/moving wedge flow problem. Of late, using Lie group analysis De *et al.*[30] investigated the heat transfer characteristics for flow past a symmetric porous wedge.

The occurrence of flow separation has several undesirable effects as it leads to an increase in the drag on a body immersed in the flow and adversely affects the heat transfer from the surface of the body. Some techniques have been developed for controlling the flow separation, viz. application of magnetic field, suction/injection at the porous wall, with the temperature-dependent fluid viscosity, etc. (Mukhopadhyay[18]).

Most of the investigations on the wedge flow problem in the literature are limited to the non-Newtonian power-law fluids. Recently, Mukhopadhyay *et al.*[31] discussed Casson fluid flow past a symmetric wedge with uniform surface temperature. To the best of the authors' knowledge, Casson fluid flow past a symmetric porous wedge with surface heat flux has not yet been addressed in the literature. Keeping this fact in mind, an attempt is made to investigate the flow and heat transfer characteristics for a Casson fluid past a symmetric wedge. With the help of similarity transformations, the governing partial differential equations corresponding to the momentum and energy equations are transformed into ordinary ones. Using the shooting method, a numerical solution of the problem is obtained. Comparisons with various previously published results in some special cases are performed and the results are found to be in excellent agreement with each other. The effects of different parameters have been studied in detail with the help of their graphical representations.

2. Formulation of the problem

We consider a steady, two-dimensional, laminar boundary-layer flow of a non-Newtonian Casson fluid past a symmetrical sharp wedge [Fig. 1] and its velocity is given by $u_e(x) = U_\infty (x/L)^m$ for $m \leq 1$ where L is a characteristic length and m is the wedge angle parameter related to the included angle $\pi\beta_1$ by $m = \beta_1/(2-\beta_1)$. It is worth mentioning that β_1 is a measure of the pressure gradient. If β_1 is positive, the pressure gradient is negative (favorable), and a negative value of β_1 denotes a positive pressure gradient (adverse). For $m < 0$, the solution becomes singular at $x = 0$, while for $m \geq 0$, the solution can be determined for all values of x.

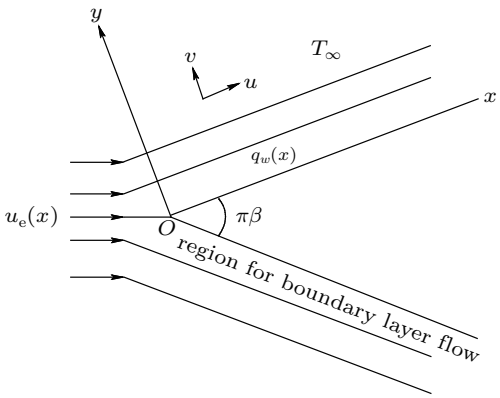


Fig. 1. Sketch of the physical problem and the coordinate system.

The rheological equation of state for an isotropic and incompressible flow of a Casson fluid is given by[32,33]

$$\tau_{ij} = \begin{cases} 2(\mu_B + p_y/\sqrt{2\pi})e_{ij}, & \pi > \pi_c, \\ 2(\mu_B + p_y/\sqrt{2\pi_c})e_{ij}, & \pi < \pi_c. \end{cases}$$

Here, $\pi = e_{ij}e_{ij}$ and e_{ij} is the (i, j)-th component of the deformation rate, π is the product of the component of deformation rate with itself, π_c is a critical value of this product based on the non-Newtonian model, μ_B is the plastic dynamic viscosity of the non-Newtonian fluid, and p_y is the yield stress of the fluid.

The governing equations of such a type of flow, in the usual notations, can be written as

$$\frac{\partial u}{\partial x} + \frac{\partial \upsilon}{\partial y} = 0, \tag{1}$$

$$u\frac{\partial u}{\partial x} + \upsilon\frac{\partial u}{\partial y} = u_e\frac{\partial u_e}{\partial x} + \nu\left(1 + \frac{1}{\beta}\right)\frac{\partial^2 u}{\partial y^2}, \tag{2}$$

$$u\frac{\partial T}{\partial x} + \upsilon\frac{\partial T}{\partial y} = \frac{\kappa}{\rho c_p}\frac{\partial^2 T}{\partial y^2}, \tag{3}$$

where the viscous dissipation term in the energy equation is neglected due to its small value for an incompressible fluid motion. Here, u and υ are the components of velocity in the x and y directions, respectively, while $\nu = \mu/\rho$ is the kinematic viscosity of the fluid, μ is the coefficient of fluid viscosity, ρ is the fluid density, β is the Casson parameter, U_∞ is the main stream velocity, T is the temperature, κ is the thermal conductivity of the fluid and c_p is the specific heat at constant pressure.

2.1. Boundary conditions

The appropriate boundary conditions for the problem are given by

$$u = 0, \quad \upsilon = -\upsilon_w(x), \quad \frac{\partial T}{\partial y} = -\frac{q_w(x)}{\kappa} \quad \text{at} \quad y = 0, \tag{4}$$

$$u = u_e(x), \quad T \to T_\infty \quad \text{as} \quad y \to \infty, \tag{5}$$

where T_∞ is the free stream or ambient temperature,

$$q_w(x) = \sqrt{\frac{(m+1)L^m}{2\nu U_\infty}}\frac{1}{q_w x^{(m-1)/2}}$$

is the variable surface heat flux, q_w being a constant,[34] $\upsilon_w(x) = \upsilon_0 x^{(m-1)/2}$, a special type of velocity at the wall which is considered with υ_0 being a constant. Here $\upsilon_w(x) > 0$ is the velocity of suction and $\upsilon_w(x) > 0$ is the velocity of blowing.

2.2. Method of solution

We now introduce the following relations for u, υ as

$$u = \frac{\partial \psi}{\partial y}, \quad \upsilon = -\frac{\partial \psi}{\partial x}, \tag{6}$$

where ψ is the stream function.

We also introduce the following variables

$$\theta(\eta) = \frac{\kappa(T - T_\infty)}{q_w}\frac{(m+1)}{2\nu}, \tag{7}$$

$$\eta = y\sqrt{\frac{(m+1)U_\infty}{2\nu L^m}}x^{(m-1)/2},$$

$$\psi = \sqrt{\frac{2\nu U_\infty}{(m+1)L^m}}x^{(m+1)/2} f(\eta). \tag{8}$$

Applying relations (6), (7), and (8) to the boundary layer equation (2) and the energy equation (3), we obtain the following equations

$$\frac{\partial \psi}{\partial y}\frac{\partial^2 \psi}{\partial x \partial y} - \frac{\partial \psi}{\partial x}\frac{\partial^2 \psi}{\partial y^2} = \frac{U_\infty^2}{L^{2m}} m x^{2m-1} + \nu\left(1 + \frac{1}{\beta}\right)\frac{\partial^3 \psi}{\partial y^3}, \tag{9}$$

$$\frac{\partial \psi}{\partial y}\frac{\partial T}{\partial x} - \frac{\partial \psi}{\partial x}\frac{\partial T}{\partial y} = \frac{\kappa}{\rho c_p}\frac{\partial^2 T}{\partial y^2}. \tag{10}$$

The boundary conditions Eqs. (4) and (5) then become

$$\frac{\partial \psi}{\partial y} = 0, \quad \frac{\partial \psi}{\partial x} = \upsilon_w, \quad \theta' = -1 \quad \text{at} \quad y = 0, \tag{11}$$

$$\frac{\partial \psi}{\partial y} = \frac{U_\infty}{L^m} x^m, \quad \theta \to 0 \quad \text{as} \quad y \to \infty. \tag{12}$$

The combination of Eqs. (8), (9), and (10) can finally yield the following form

$$\left(1 + \frac{1}{\beta}\right) f''' + f f'' + \frac{2m}{m+1}(1 - f'^2) = 0, \tag{13}$$

$$\frac{1}{Pr}\theta'' + f\theta' = 0, \tag{14}$$

and the boundary conditions finally become

$$f'(\eta) = 0, \quad f(\eta) = S, \quad \theta' = -1, \quad \text{at} \quad \eta = 0, \tag{15}$$

$$f'(\eta) = 1, \quad \theta \to 0 \quad \text{as} \quad \eta \to \infty, \tag{16}$$

where $Pr = \mu c_p/\kappa$ is the Prandtl number and $S = \sqrt{2}\upsilon_0/\sqrt{\nu U_\infty (m+1)}$ is the suction/blowing parameter.

Equations (13) and (14) along with the boundary conditions are solved by converting them into an initial value problem. We set

$$f' = z, \quad z' = p, \quad p' = \left\{\frac{2m}{m+1}\left(z^2 - 1\right) - fp\right\} \Big/ \left(1 + \frac{1}{\beta}\right), \tag{17}$$

$$\theta' = q, \quad q' = -Prfq, \tag{18}$$

with the boundary conditions

$$f(0) = S, \quad f'(0) = 0, \quad \theta'(0) = -1. \tag{19}$$

In order to integrate Eqs. (17) and (18) as an initial value problem, we require values for $p(0)$ (that is, $f''(0)$) and $q(0)$ (that is, $\theta(0)$) but no such values are given in the boundary conditions. The suitable guess values for $f''(0)$ and $\theta(0)$ are chosen and then integration is carried out.[35] We compare the calculated values for f' and θ at $\eta = 8$ (say) with the results obtained in the given boundary condition $f'(8) = 1$ and $\theta(8) = 0$ and adjust the estimated values, $f''(0)$ and $\theta(0)$, to give a better approximation for the solution. We take the series of values for $f''(0)$ and $\theta(0)$, and use the fourth-order classical Runge–Kutta method in steps of $h = 0.01$. The above procedure is repeated until we obtain the converged results within a tolerance limit of 10^{-5}.

For the verification of the accuracy of the applied numerical scheme, results for $f''(0)$ for various values of m in the case of a Newtonian fluid are compared with those reported by Yih,[14] Chamkha *et al.*,[16] Pal and Mondal,[19] and Cebeci and Bradshaw.[36] The results are found to be in excellent agreement which builds confidence that the present numerical results are accurate and the numerical method used is accurate. The comparisons are shown in Table 1.

Table 1. Comparison among the values of $f''(0)$ for variable values of m for Newtonian fluid.

m	Yih[14]	Chamkha *et al.*[16]	Pal and Mondal[19]	Cebeci and Bradshaw[36]	Present study
−0.05	0.213484	0.213802	0.213484	0.21351	0.213802
0	0.332057	0.332206	0.332206	0.33206	0.332206
0.33	0.757448	0.757586	0.757586	0.75745	0.757586
1	1.232588	1.232710	1.232710	1.023259	1.232710

3. Results and discussion

In order to analyze the results, numerical computation is carried out for various values of the Falkner–Skan exponent m, Casson fluid parameter β, suction/blowing parameter S, and the Prandtl number Pr. For illustrations of the results, numerical values are plotted in Figs. 2–6.

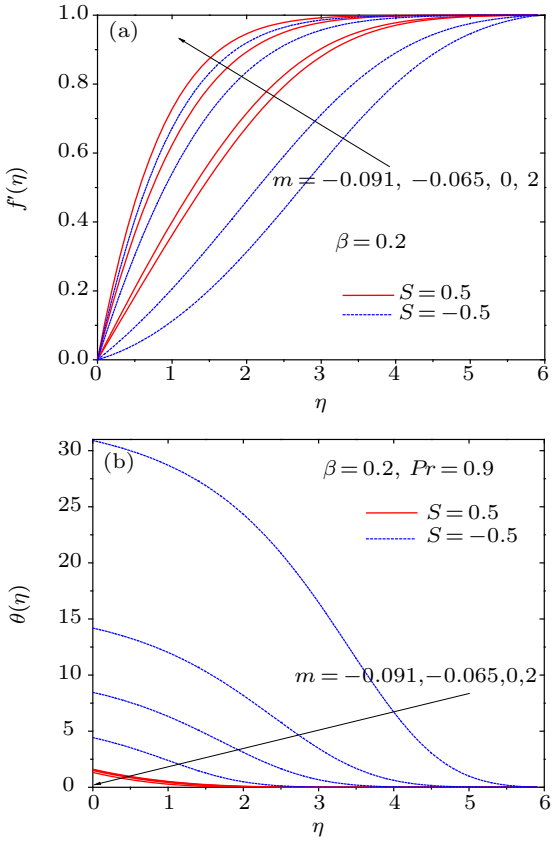


Fig. 2. (color online) Velocity (a) and temperature (b) profiles for variable values of m.

Figures 2(a) and 2(b) depict the effects of the Falkner–Skan exponent m on the velocity and temperature profiles in the presence of suction/blowing, respectively. Figure 2(a) presents the effects of increasing m on fluid velocity. With the increasing value of exponent m, the fluid velocity is found to increase. It is observed that in the case of an accelerated flow ($m > 0$), the velocity profiles have no point of inflection for both cases of suction and blowing whereas in the case of decelerated flow ($m < 0$), they exhibit a point of inflection which is observed in the presence of blowing ($S = -0.5$) only and flow separation occurs at $m = -0.091$. No point of inflection is seen in the case of suction ($S = 0.5$). For accelerated flows (i.e. positive values of m), the velocity profiles merely squeeze closer and closer to the wall, and backflow phenomena are not observed. Here, $m = 0$ presents the result for a flat plate. It is seen that the boundary layer thickness decreases as m increases, hence it gives rise to the velocity gradient, which in turn causes an increase in skin friction [Fig. 2(a)]. Figure 2(b) exhibits that the temperature $\theta(\eta)$ in the boundary layer region decreases with the increasing value of m. Temperature at a point is higher in the case of blowing than in the case of suction. Temperature variation is more pronounced in the case of blowing. Since the thermal boundary layer thickness increases with the increasing value of m, it causes a decrease in the rate of heat transfer [Fig. 2(b)].

The effects of the Casson fluid parameter β on the velocity and temperature profiles in the absence/presence of suction/blowing are exhibited in Figs. 3(a)–3(e), respectively. From all the figures it is very clear that with the increasing value of β, fluid velocity increases but the temperature is found to decrease. Figure 3(a) clearly indicates that the thickness of the velocity boundary layer decreases. No point of inflection is observed for higher values of β [see Figs. 3(a) and 3(c)]. From these figures, it is very clear that the flow separation can be controlled in the case of a non-Newtonian Casson fluid by increasing the value of the Casson fluid parameter. Figures 3(d) and 3(e) show that the temperature decreases with the increasing value of β. That is, the rate of heat transfer (the thermal boundary layer thickness becomes thinner) is enhanced when the velocity boundary layer thickness decreases.

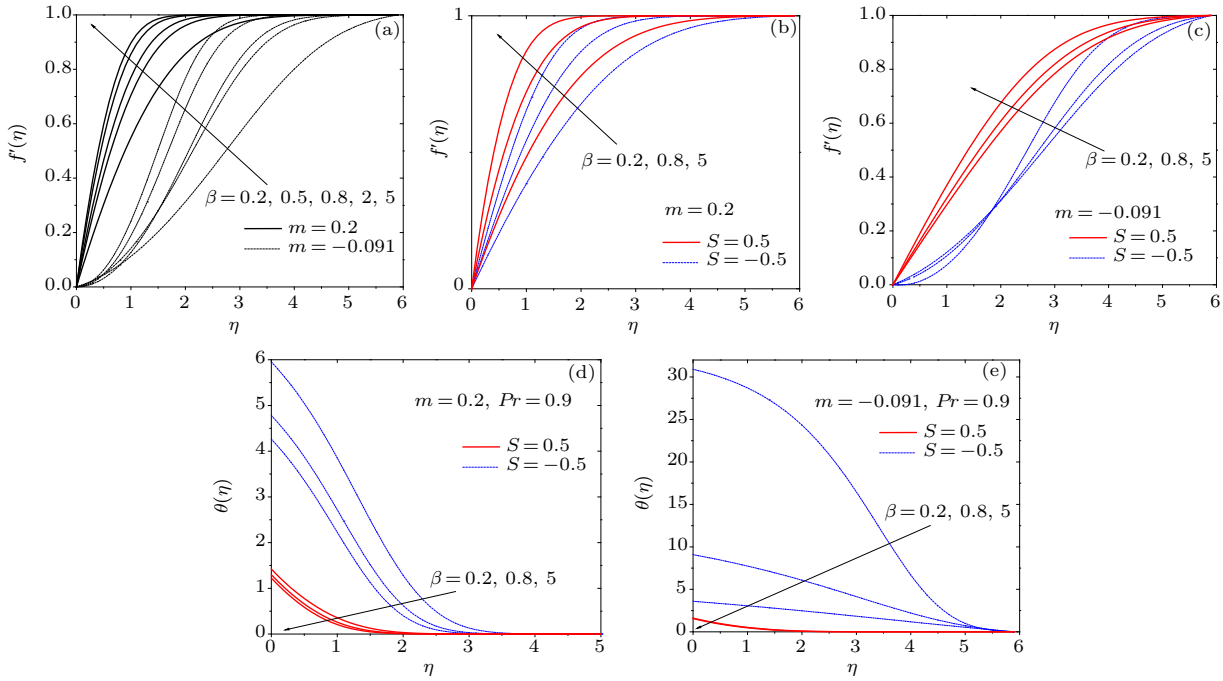


Fig. 3. (color online) Velocity profiles for variable values of Casson parameter β (a) in the absence of suction/blowing, (b) for accelerated flow, (c) for decelerated flow; temperature profiles for variable values of Casson parameter β (d) for accelerated flow, and (e) for decelerated flow.

Figures 4(a) and 4(b) depict respectively the natures of velocity and temperature profiles for various values of suction/blowing parameter S. Fluid velocity increases with the increasing value of suction/blowing parameter S [Fig. 4(a)] whereas temperature decreases with the increasing value of S [Fig. 4(b)]. The explanation for such a behavior is that the fluid is brought closer to the surface and reduces the thermal boundary layer thickness. The thermal boundary layer thickness increases with injection which causes a decrease in the rate of heat transfer. Point of inflection is observed only in the case of blowing [Fig. 4(a)] and flow separation is controlled in the case of suction [Fig. 4(a)].

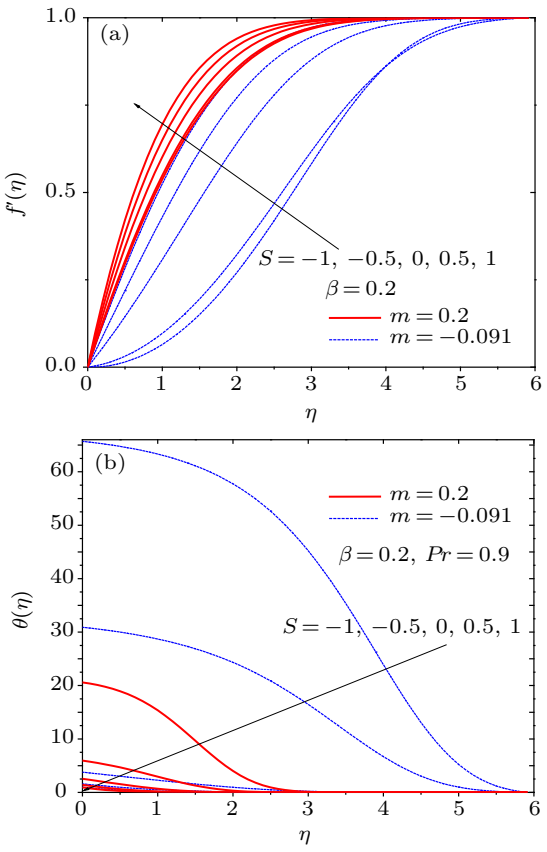


Fig. 4. (color online) Velocity (a) and temperature (b) profiles for variable values of suction/blowing parameter S.

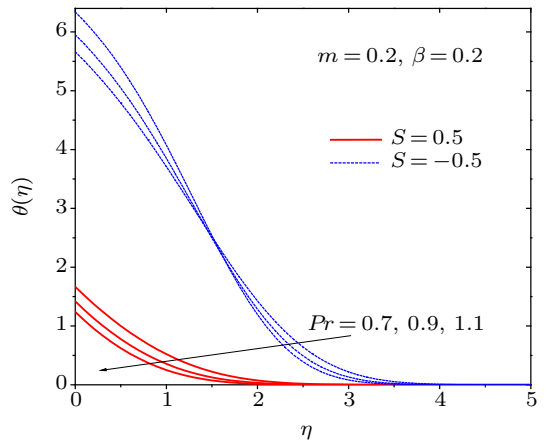


Fig. 5. (color online) Temperature profiles for variable values of Prandtl number Pr.

Figure 5 presents the effect of the Prandtl number on the temperature profile. With the increasing value of the Prandtl number Pr, the temperature is found to decrease. This is in agreement with the physical fact that the thermal boundary layer thickness decreases with the increasing value of Pr.

Figure 6 exhibits the nature of the skin friction coefficient. It is very clear that the force due to the skin friction increases as the included angle of the wedge (β_1) increases, i.e. the skin friction coefficient increases with the increase of Falkner–Skan exponent m but it decreases with the increasing Casson fluid parameter β.

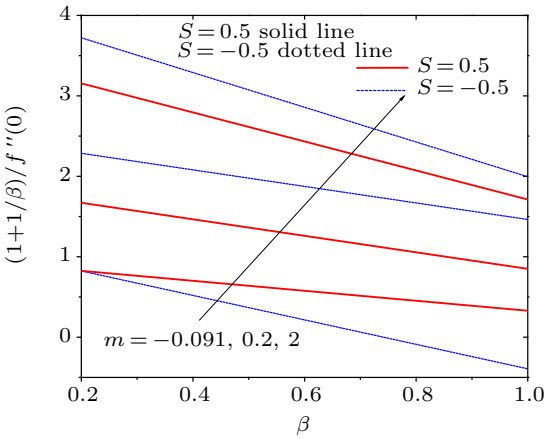


Fig. 6. (color online) Variations of skin friction coefficient with Casson parameter β for various values of m.

4. Conclusions

Heat transfer characteristics for boundary layer flow of a Casson fluid over a symmetric porous wedge with surface heat flux is presented. A transformed set of self-similar equations is obtained. The reduced equations are then solved numerically by the Runge–Kutta method with the help of the shooting technique. Fluid velocity is found to increase with the increasing Casson fluid parameter whereas the temperature decreases in this case. The non-dimensional temperature decreases with the increasing value of Prandtl number. A significant result obtained is that by increasing the value of the Casson fluid parameter as well as by increasing the strength of the applied suction, flow separation can be prevented. The rate of heat transfer increases with the increasing values of Falkner–Skan exponent, Casson fluid parameter, and Prandtl number.

Acknowledgment

One of the authors (Swati Mukhopadhyay) thanks the UGC, New Delhi, India for the financial support under the Special Assistance Programme DSA Phase-1.

References

[1] Mukhopadhyay S 2012 *Z. Naturforsch* **67a** 641 DOI: 10.5560/ZNA.2012-0075
[2] Mukhopadhyay S and Vajravelu K 2012 *ASME J. Appl. Mech.* **79** 044508-1
[3] Mukhopadhyay S 2012 *Chin. Phys. Lett.* **29** 054703

[4] Mukhopadhyay S and Bhattacharyya K 2012 *J. Egyptian Math. Soc.* **20** 229
[5] Patel V and Timol M G 2012 *Int. J. Appl. Math. Mech.* **8** 77
[6] Eldabe N T M and Salwa M G E 1995 *J. Phys. Soc. Jpn.* **64** 41
[7] Dash R K, Mehta K N and Jayaraman G 1996 *Int. J. Engng. Sci.* **34** 1145
[8] Falkner V M and Skan S W 1931 *SIAM J. Appl. Math.* **49** 1350
[9] Hartree D R 1937 *Proc. Cambridge Phil. Soc.* **33** 223
[10] Hady F M and Hassanien I A 1985 *Astrophys. Space Sci.* **112** 381
[11] Lin H T and Lin L K 1987 *Int. J. Heat Mass Transfer* **30** 1111
[12] Watanabe T and Pop I 1993 *Int. Commun. Heat Mass Transfer* **20** 871
[13] Kafoussias N G and Nanousis N D 1997 *Can. J. Phys.* **75** 733
[14] Yih K A 1996 *Int. Commun. Heat Mass Transfer* **26** 819
[15] Hossain M A, Munir M S and Rees D A S 2000 *Int. J. Thermal Sci.* **39** 635
[16] Chamkha A J, Quadri M M and Camille I 2003 *Heat Mass Transfer* **39** 305
[17] Pantokratoras A 2006 *Int. J. Thermal Sci.* **45** 378
[18] Mukhopadhyay S 2009 *J. Appl. Fluid Mech.* **2** 29
[19] Pal D and Mondal H 2009 *Appl. Math. Comput.* **212** 194
[20] Kandasamy R, Periasamy K and Sivagnana Prabhu K K 2005 *Int. J. Heat Mass Transfer* **48** 1388
[21] Hossain M A, Bhowmik S and Gorla R S R 2006 *Int. J. Engng. Sci.* **44** 607
[22] Kim Y J 1999 *Acta Mech.* **138** 113
[23] Kim Y J and Kim T A 2003 *Int. J. Appl. Mech. Engng.* **8** 147 Special issue: ICER 2003
[24] Ishak A, Nazar R and Pop I 2009 *Commun. Nonlinear Sci. Numer. Simul.* **14** 109
[25] Riley N and Weidman P D 1989 *J. Appl. Math. Comput.* **25** 67
[26] Ishak A, Nazar R and Pop I 2006 *Int. J. Engng. Sci.* **44** 1225
[27] Ishak A, Nazar R and Pop I 2007 *J. Appl. Math. Comput.* **25** 67
[28] Kandasamy R, Muhaimin, Hashim I and Ruhaila 2008 *Nuclear Engng. Design* **238** 2699
[29] Yacob N A, Ishak A and Pop I 2011 *Int. J. Thermal Sci.* **50** 133
[30] De P R, Mukhopadhyay S and Layek G C 2012 *Acta Technica* **57** 227
[31] Mukhopadhyay S, Mondal I C and Chamkha A J 2013 *Heat Transfer — Asian Research* **48** 665
[32] Bhattacharyya K, Hayat T and Alsaedi A 2013 *Chin. Phys. B* **22** 024702
[33] Mukhopadhyay S 2013 *Chin. Phys. B* **22** 074701
[34] Ishak A, Pop I and Nazar R 2009 *Chin. Phys. Lett.* **26** 014702
[35] Mondal I C and Mukhopadhyay S 2012 *Ain Shams Engng. J.* doi:10.1016/j.asej.2012.06.004
[36] Cebeci T and Bradshaw P 1984 *Physical and Computational Aspect of Covective Heat Transfer* (New York: Springer-Verlag)